THE JOURNAL OF PHYSICAL CHEMISTRY B

Article

pubs.acs.org/JPCB

Visible-Light Photocatalyzed Cross-Linking of Diacetylene Ligands by Quantum Dots to Improve Their Aqueous Colloidal Stability

Marion G. Götz,[†] Hiroko Takeuchi,[‡] Matthew J. Goldfogel,[†] Julia M. Warren,[†] Brandon D. Fennell,[†] and Colin D. Heyes*[,‡]

[†]Department of Chemistry, Whitman College, 345 Boyer Avenue, Walla Walla, Washington 99362, United States

[‡]Department of Chemistry and Biochemistry, University of Arkansas, 345 North Campus Drive, Fayetteville, Arkansas 72701, United States

Supporting Information

ABSTRACT: Ligand cross-linking is known to improve the colloidal stability of nanoparticles, particularly in aqueous solutions. However, most cross-linking is performed chemically, in which it is difficult to limit interparticle cross-linking, unless performed at low concentrations. Photochemical cross-linking is a promising approach but usually requires ultraviolet (UV) light to initiate. Using such high-energy photons can be harmful to systems in which the ligand−nanoparticle bond is fairly weak, as is the case for the commonly used semiconductor quantum dots (QDs). Here, we introduce a novel approach to cross-link thiolated ligands on QDs by utilizing the photocatalytic activity of QDs upon absorbing visible light. We show that using visible light leads to better ligand cross-linking by avoiding the problem of ligand dissociation that occurs upon UV light exposure. Once cross-linked, the ligands significantly enhance the colloidal stability of those same QDs that facilitated cross-linking.

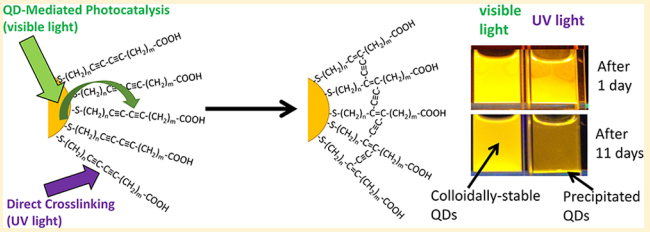

INTRODUCTION

The synthesis of high-quality colloidal core−shell quantum dots (QDs) is usually performed in organic solvents.[1−3] From these solvents, they can be processed and used in numerous applications in optoelectronics[4−7] and photovoltaics.[8] Alternatively, the QDs can be subsequently transferred into aqueous solutions in order to increase their range of applications, particularly in biological labeling[9−11] and environmental sensing.[12,13] Such a transfer requires either hydrophilic bifunctional ligands to be exchanged for the native hydrophobic monofunctional coordinating ligands, usually octadecylamine (ODA)[10,14] or the addition of amphiphilic ligands or diblock copolymers where the hydrophobic regions intercalate with the native ligands and hydrophilic regions are exposed to the aqueous environment.[15,16] There are advantages and disadvantages to each approach,[17−19] but it mainly comes down to a choice of size vs stability. The long-chain native ligands and the amphiphilic nature of ligands used in the intercalation approach lead to QDs with relatively large overall diameters. The ligand-exchange approach can, in principle, use extremely small ligands. However, when using these QDs for fluorescence applications, it has been found that fluorescence quenching depends on both ligand size and the functional group used,[20] so a balance is usually found between size, stability, and fluorescence quantum yield. As a compromise, small polydentate ligands such as dihydrolipoic acid (DHLA) have been used to improve colloidal stability over monodentate ligands,[21] although we have recently found that the lower density of DHLA ligands on the surface compared to monodentate MPA ligands leads to higher nonspecific adsorption of target thiol molecules at low concentrations.[22] In any case, the colloidal stability of ligand-exchanged quantum dots is usually lower than the amphiphilic polymer-coated QDs and depends strongly on the nature of the ligands and the solvent conditions. This can be a particularly significant problem at low QD concentration and under reductive or oxidative conditions,[23,24] as is often the case in biological fluorescence labeling applications.

Combining the advantages of ligand exchange using compact, water-soluble ligands with cross-linking has the potential to allow a better compromise in which the size increase is modest while the improvement in colloidal stability should be significant. Only a few examples of cross-linking compact, ligand-exchanged QDs have been reported, and they have used a chemical cross-linking approach.[25,26] However, a major disadvantage with chemical cross-linking is that it is difficult to inhibit interparticle cross-linking, which means that a purification step may be required and overall yield will be compromised. Photochemical cross-linking is an attractive alternative to localize the cross-linking to within a particle, particularly if the cross-linking group is not exposed to the solvent environment. Self-assembled monolayers (SAMs) of diacetylene ligands on gold were directly photo-cross-linked

Special Issue: Spectroscopy of Nano- and Biomaterials Symposium

Received: May 30, 2014
Revised: July 12, 2014
Published: July 18, 2014

   dx.doi.org/10.1021/jp505340c | J. Phys. Chem. B 2014, 118, 14103−14109

Scheme 1. Ligand Exchange and Photocatalyzed Polymerization of Diacetylene Ligands on Quantum Dots Using Either UV Light or Visible Light

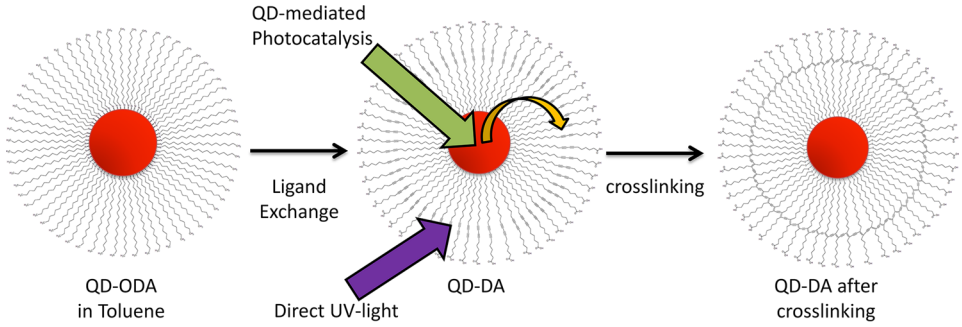

using high-energy ultraviolet light (UV, 254 nm) and were shown to result in surfaces that are extremely robust for use in harsh environments.[27,28] In this study, we demonstrate that QDs themselves can initiate cross-linking of bifunctional diacetylene ligands using lower energy visible light to generate radicals (Scheme 1). Photoexcited CdSe has been previously used to generate radicals on adsorbed species for charge separation in photovoltaic applications[29] and in solid-state polymer−nanocomposite blends.[30,31] However, to the best of our knowledge, using a QD-mediated photo-cross-linking approach in solution to limit interparticle cross-linking while, at the same time, promoting intraparticle cross-linking to improve the colloidal stability of those same QDs has not yet been demonstrated. We show that taking advantage of the QD as a visible-light initiator leads to much better cross-linking of the ligands than direct cross-linking of the diacetylene groups with UV light, since competing ligand dissociation reactions induced by UV exposure are avoided. Our approach results in extensive intraparticle cross-linking but with practically no interparticle cross-linking, and more importantly, it leads to excellent long-term colloidal stability of the QDs in aqueous environments while maintaining relatively small hydrodynamic sizes.

EXPERIMENTAL SECTION

Synthesis of Diacetylene Ligand. The synthesis of the bifunctional diacetylene (DA) ligand followed a combination of procedures described by Xu et al.[32] and Kim et al.[33] Details of the DA ligand synthesis and NMR peak assignments are provided in the Supporting Information.

Ligand Exchange of QD-ODA with MPA (QD-MPA) and Diacetylene (QD-DA) Ligands. CdSe/ZnS (core/shell) quantum dots (λ_{em} = 597 nm) coated with hydrophobic octadecylamine (ODA) ligands were purchased from Ocean NanoTech (Springdale, AR) as a dried powder and dissolved in toluene (EMD Chemicals Inc., Billerica, MA). Prior to the ligand exchange procedure, the as-purchased QDs were purified from excess ligands by precipitating from toluene with acetone (EMD), centrifuging at 14 100*g* (14 500 rpm, MiniSpin plus, Eppendorf), and discarding the supernatant. Then, the precipitated QDs were redissolved into chloroform (DriSolv, EMD), mixed with methanol (EMD), and centrifuged again and the supernatant was discarded. A ligand solution was prepared by adding 10 mg of the DA ligand to 1 mL of chloroform or by adding 2.66 μL of mercaptopropanoic acid (MPA) (Alfa Aesar, Ward Hill, MA) in 1 mL of methanol. The pH was adjusted to 11 by adding microliter quantities of a stock solution of tetramethylammonium hydroxide (TMAOH) (Alfa Aesar) in methanol. The ligand solution was added to the precipitated QDs, and stirred for 24 h at room temperature in the dark.

Photopolymerization of Diacetylene Ligands on QD-DA. It has been shown that 254 nm UV exposure can be used to photopolymerize diacetylenes.[27] The fluorescence of the sample as a function of 254 nm (short wave) UV exposure time was monitored to determine the optimal cross-linking time in terms of the fluorescence properties. Emission spectra were obtained by exciting at 530 nm in a 100 μL quartz fluorescence cuvette (Starna Cells). From all the samples, those exposed for 0, 20, 100, and 210 min were then analyzed with an FT-IR spectrometer (Bruker, Vertex 70) equipped with a DTGS detector. A 40 μL aliquot of the sample was taken from the stock solution at the specified time of exposure and placed in the exact center of a CaF_2 window which was then left to dry under a N_2 atmosphere so that the IR beam diameter completely probed the whole sample spot. A total of 16 scans were averaged to obtain the spectra.

Phase Transfer of QD-DA and QD-MPA to Water. To transfer the water-soluble QD-DA and QD-MPA to water, methanol and acetone were added, respectively, and the mixture was centrifuged to precipitate the QDs from the reaction solution. Having removed the supernatant, the QDs were redissolved into Millipore (18.2 MΩ·cm) water. Each solution was transferred to a four-windowed quartz fluorescence cuvette with a stopper (Starna) for further analysis.

Characterization of QD-DA and QD-MPA in Aqueous Solutions. Photographs to show QD fluorescence and colloidal dispersion in water were taken with a 10.1 MP camera (Pentax) whereby a hand-held UV lamp operating at 366 nm (long wave) was shone from beneath the four-windowed quartz fluorescence cuvettes containing the samples. Absorption spectra were taken in this same cuvette using a Hitachi U3900H spectrometer. Single particle burst analysis and fluorescence lifetimes were acquired on a Picoquant Microtime 200 fluorescence microscope as previously described.[34,35] A pulsed laser operating at 485 nm, 15 μW, and 5 MHz was used for excitation and focused though the objective (PlanApo 63xW, Olympus) to a diffraction-limited spot. The emission was collected by the same objective and passed through a 100 μm pinhole and a 585/55m filter before being detected on a Single Photon Counting Avalanche Diode (PDM series, Microphotonic devices, Bolzano, Italy), and the data was saved in time-tagged time-resolved format to enable offline calculation of fluorescence bursts, fluorescence lifetime, and fluorescence correlation spectroscopy (FCS) using the SymPhoTime software (version 5.3.2, Picoquant GmbH).

dx.doi.org/10.1021/jp505340c | J. Phys. Chem. B 2014, 118, 14103−14109

RESULTS AND DISCUSSION

The absorption and photoluminescence (PL) spectra of the QDs before ligand exchange (QD-ODA) and after (QD-MPA, or QD-DA) are shown in Figure 1. In addition to the

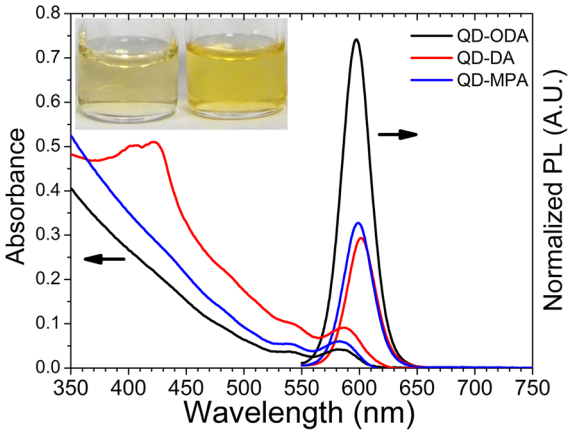

Figure 1. Absorption and photoluminescence spectra of QDs before (black) and after ligand exchange with MPA (blue) and DA (red). Inset: photographs of QDs under room light after ligand exchange using MPA (left) and DA (right) show relative solubilization efficiency.

characteristic QD exciton absorbance peak at 583 nm and the broad absorbance that increases with increasing energy that is observed in each sample, the absorbance of QD-DA shows another intense peak between 400 and 430 nm, which is assigned to $\pi-\pi^*$ transitions in the diacetylene moiety. It was found that using the same initial QD concentration for the ligand exchange resulted in better solubilization efficiency compared to QD-MPA, as evidenced by the stronger color of the solutions shown in the inset of Figure 1. This could be a consequence of the diacetylene ligands favoring a close-packing arrangement on the QD surface, resulting in a SAM-driven ligand exchange process, whereby hydrophobic interactions between chains result in a higher ligand density compared to the shorter and more soluble (i.e., labile) MPA ligands. In both cases, however, the fluorescence quantum yield decreased by approximately half, which is common for thiolated ligands on QDs—even those with a core−shell configuration.[20] The DA ligands decreased the quantum yield a little more than MPA, consistent with a more complete ligand exchange (more thiols) because of SAM packing.

We hypothesized that using high-energy UV light to directly photo-cross-link diacetylene ligands on QDs would not be ideal, since the QD−thiol coordination bond would be prone to photooxidation[20,36] but that QDs excited with visible light could be used to initiate photo-cross-linking. To test our hypothesis, we measured the absorption spectra of QD-DA in water as a function of time left exposed to room light. One QD-DA sample was first exposed to 30 min of UV light, while the other was not. This data is presented in parts a and b of Figure 2, respectively. At day 0, the characteristic diacetylene peak between 400 and 430 nm was stronger for the unexposed QD-DA compared to the UV-exposed QD-DA. This could be a consequence of DA ligands undergoing partial cross-linking and/or UV-induced dissociation (*vide infra*). As the QDs were left exposed to room light for up to 2 weeks, significant changes in the absorption spectra were observed for both samples, although the details are somewhat different. Both samples show

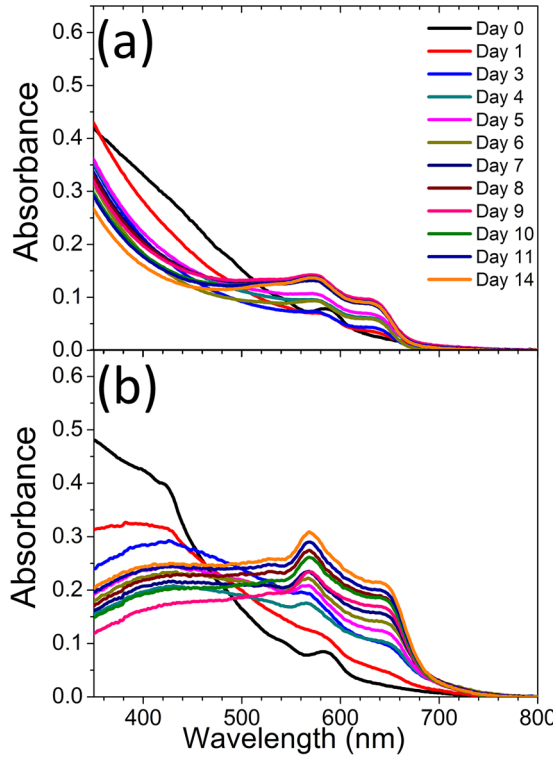

Figure 2. UV−vis absorption spectra of QD-DA in water as a function of exposure to room light over a 2-week period that (a) had been and (b) had not been exposed to 30 min of UV light prior to transfer to water.

the formation of a new peak at ∼650 nm, which begins to form within the first day and increases steadily. This increase is concomitant with a decrease in the absorbance in the 350−450 nm region. We assign this 650 nm peak to $\pi-\pi^*$ transition of the long, conjugated π-electron system that results from extensive cross-linking of the DA ligands on the QD induced by visible light. A similar peak has also been observed for similar ligands on gold particles that were irradiated with UV light for 30−120 min.[28] In the case of the QDs studied here, QD-DA that had been exposed to UV light first showed an increase in the 650 nm peak within 7 days and then saturated, indicating that cross-linking stopped prematurely. For the QD-DA samples that had not been exposed to UV light first, the 650 nm peak continued to increase for the full 14 days and the decrease in the 350−450 nm region was much more pronounced, suggesting that visible-light-induced cross-linking was slower but more extensive, without the competing process of UV-induced ligand dissociation that prematurely halts cross-linking. In both cases, the excitonic QD peak at 583 nm showed a moderate blue-shift: to 572 nm in the case of UV-exposed QD-DA and to 568 nm for the non-UV-exposed QD-DA. It is interesting to note that, for the UV-exposed samples on day 0, the peak at 650 nm was absent, suggesting that the UV exposure was not able to induce much conjugation even though the 400−430 nm peak was attenuated. This is consistent with our interpretation of a competition between UV-induced cross-linking and ligand dissociation which limits the extent of cross-linking that can occur. Such a competition was probably not observed in the case of gold,[28] since UV light does not excite gold as it does for semiconductor QDs and UV-induced ligand dissociation does not occur for the stable Au−S bond.

dx.doi.org/10.1021/jp505340c | J. Phys. Chem. B 2014, 118, 14103−14109

Further evidence that UV light leads to only partial cross-linking of QD-DA and competing UV-induced dissociation of the DA ligands from the QD is found using FT-IR spectroscopy. Figure 3 shows the FT-IR transmittance spectra

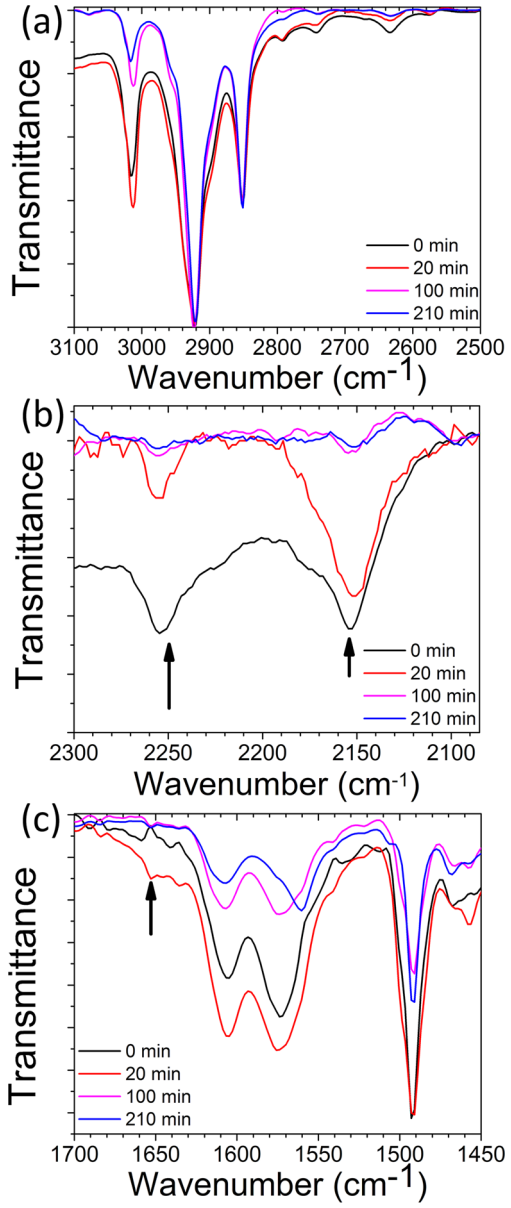

Figure 3. FT-IR transmittance spectra of QD-DA as a function of UV exposure time showing (a) C—H stretching, (b) C≡C stretching, and (c) C═C and C═O stretching, as well as C—H bending modes.

in three regions of interest as a function of exposure time to UV light. In Figure 3a, the 3100–2500 cm^{-1} region shows the sp^3 C—H stretching peaks and the asymmetric stretch at 2922 cm^{-1} is used to normalize the spectra. It can be seen that, as expected, the symmetric sp^3 C—H stretch at 2850 cm^{-1} also did not change. The peak at 3012 cm^{-1} first increased slightly and then decreased upon UV exposure. This peak is usually assigned to alkenyl C—H peaks from C═C bonds. However, cross-linking of diacetylenes should not result in such a peak, unless side-reactions occurred that led to incomplete cross-linking. This may be possible if there was no adjacent diacetylene to cross-link to, due to partial ligand removal, leaving a reactive C═C radical that may have led to the formation of a —C═C—H bond. Figure 3b shows the 2100–2300 cm^{-1} region as a function of exposure time of the QD-DA to UV light, where C≡C bonds have a weak but isolated absorbance. In fact, two peaks are observed in this region, one at 2153 cm^{-1} and another at 2254 cm^{-1} (black arrows), which are characteristic of diacetylenes.[37] After 20 min of UV exposure, the 2254 cm^{-1} peak effectively disappeared, while the 2153 cm^{-1} peak diminished only slightly. Within 100 min of exposure, both peaks disappeared. As expected from the cross-linking reaction (Scheme 1),[27] the —C≡C—C≡C— moieties become $(—C═C—C≡C—)_n$, and the change from a double peak to a single peak within 20 min may reflect this. However, the fact that both peaks decreased within 100–210 min suggests that neither type of ligand was present on the particles after extended UV exposure. Figure 3c highlights the 1450–1700 cm^{-1} region, which shows peaks related to C═C and C═O stretching as well as C—H bending modes. The peaks at 1573 and 1604 cm^{-1} are assigned as stretches from the C═O group from deprotonated and protonated carboxylic acids, respectively, forming a close-packed hydrogen-bonded network of ligands. The peak at 1492 cm^{-1} is most likely from C—H bending modes, which remained constant within 20 min of UV exposure and reduced in the 20–100 min time window. Since the C—H stretching frequency was normalized, this reduction may indicate a significant change in the ligand arrangement on this time scale that partially reduces the oscillator strength of bending modes, which could be the result of the cross-linking process increasing the rigidity of the SAM. A small peak at 1652 cm^{-1} appearing after 20 min of UV exposure (black arrow), which was not present before cross-linking, may also be indicative of C═C bonds forming during cross-linking, but due to several overlapping peaks in this region, it is difficult to make a definitive assignment at this point. The FT-IR data can be summarized as follows: changes in the diacetylene peaks show that the UV light caused these groups to react within 20 min and that they are completely gone within 100 min. These changes were also accompanied by small increases in peaks associated with alkenyl C—H and C═C bonds in 20 min that then decreased within 100 min, suggesting side reactions limited the extent of cross-linking. In the 0–20 min time period, the C═O peaks remained but also started to decrease in the 20–100 min period. Finally, changes in the C—H bending modes suggest significant ligand rearrangement on this 20–100 min time scale. Taken together, the FT-IR data supports the fact that diacetylenes can be partially cross-linked on QD-DA within 20 min of UV exposure, but more complete cross-linking using UV light was inhibited by the fact that there was a competing process of ligand rearrangement and dissociation that took over on the 20–100 min time scale of UV exposure.

The photoluminescence intensity as a function of time exposed to UV and visible light (sequentially) is presented in the Supporting Information, which shows the effect of these partial cross-linking and ligand dissociation processes on the PL properties. This data provides more evidence that the cross-linking mechanism can be initiated using both UV and visible light and that radicals can actually improve the PL of the QDs, in agreement with a recent study,[38] but that continued exposure to UV light is extremely detrimental to the particles. In a previous study,[38] radicals were generated by external initiators to improve the PL of the QDs, but the supplementary PL data

dx.doi.org/10.1021/jp505340c | J. Phys. Chem. B 2014, 118, 14103–14109

here shows that radicals generated by the photoexcitation of QDs themselves can have a similar effect.

The significant advantage of using visible-light QD-mediated photocatalysis for cross-linking rather than UV light is highlighted in Figure 4. Photographs of the fluorescence from

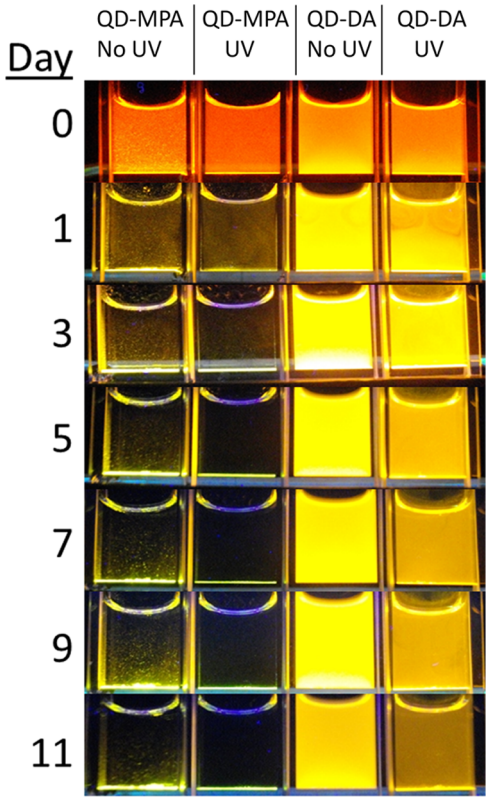

Figure 4. Fluorescence photographs under 366 nm (long wave) UV light of QD-MPA and QD-DA samples that either were or were not exposed to 30 min of 254 nm (short wave) UV light first to show colloidal stability and fluorescence intensity as a function of time. A fluorescence layer at the bottom of the vial indicated extensive aggregation of the QDs. Only the non-UV-exposed QD-DA samples show no visible aggregation over time.

QD-DA with or without 30 min prior exposure to UV light dispersed in water and then exposed to room light were taken over several days. As a comparison, QDs solubilized with one of the most commonly used, non-cross-linking thiolated ligands, QD-MPA, is shown. QD-MPA showed extensive precipitation from solution even after the first day and the effect was worsened by prior UV exposure, which would be expected for a UV-induced ligand dissociation process.[20,36] Both the QD-DA samples showed significant improvement in colloidal stability over QD-MPA. However, the non-UV-exposed QD-DA showed better long-term stability than the UV-exposed QD-DA, highlighted by the fact that the particles remained suspended in solution for the whole time period. The UV-exposed QD-DA began to precipitate from solution within 5−7 days, and by day 11 was considerably worse than the non-UV-exposed QD-DA.

The degree of aggregation or dispersion in UV-exposed and non-UV-exposed QD-DA was then analyzed using single particle fluorescence spectroscopy on a Picoquant Microtime 200 fluorescence confocal microscope,[14,35] after being left in aqueous solution for 14 days under room light. Samples were stirred and diluted to pM concentrations and analyzed using burst integrated fluorescence and fluorescence correlation spectroscopy (FCS), the results of which are shown in Figure 5.

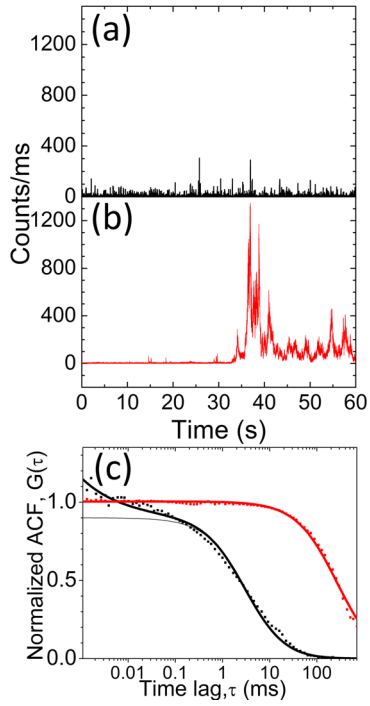

Figure 5. Example burst integrated fluorescence traces of particles diffusing through the confocal volume of a fluorescence microscope for (a) visible-light-exposed (black) and (b) UV-light-exposed (red) QD-DA, obtained after they have been sitting in water for 14 days and (c) FCS autocorrelation analysis of each QD-DA sample to show average diffusion times of particles through the confocal volume. For the non-UV-exposed QD-DA, fitted curves with (thick black) and without (thin black) taking blinking into account are included, with both fits recovering at the same diffusion times. Blinking is not needed to be taken into account for UV-exposed QD-DA (red) due to aggregation.

Figure 5a shows an example of a burst integrated fluorescence trace from visible-light-exposed QD-DA, while Figure 5b shows an example from UV-exposed QD-DA. The data is binned into 1 ms time points, with the intensity of each point corresponding to the average detector count rate during that 1 ms time bin. The peaks in fluorescence intensity arise from fluorescent particles diffusing through the diffraction-limited focused laser beam; a single peak corresponding to a single particle diffusing through the focus. The non-UV-exposed samples show much lower intensity bursts, with each peak being narrow, compared to the wide, intense peaks from the UV-exposed samples. These intense, wide peaks are due to large, highly fluorescent aggregates of QDs slowly diffusing through the laser focus. The average diffusion time of particles diffusing through the focus is analyzed by calculating the autocorrelation function (ACF) from the burst integrated fluorescence traces, which is shown in Figure 5c. The black curve shows the ACF for the non-UV-exposed QD-DA, while the red curve shows UV-exposed QD-DA. The diffusion coefficients are calculated by fitting these curves to extract diffusion times through the confocal volume. The data were fit to eq 1, to take blinking into account as previously described.[39]

dx.doi.org/10.1021/jp505340c | J. Phys. Chem. B 2014, 118, 14103−14109

$$G(\tau) = G_{\mathrm{Diff}}(\tau)\left(1 + \frac{F(A\cdot\tau^{\alpha-2})}{1-F}\right) \quad (1)$$

where

$$G_{\mathrm{Diff}}(\tau) = G(0)\left(\frac{1}{1+\frac{\tau}{\tau_{\mathrm{D}}}}\right)\left(\frac{1}{\sqrt{1+\left(\frac{w_0}{z_0}\right)^2+\frac{\tau}{\tau_{\mathrm{D}}}}}\right) \quad (2)$$

With w_0 and z_0 describing the width (500 nm) and height (2 μm) of the confocal beam, F describes the fraction of particles that blinked during the transit time in the beam and A and α describe the power-law blinking dynamics, as previously described.[39,40] Fits both with and without taking blinking into account were performed (i.e., either by setting $F = 0$ or allowing it to be fit). For the non-UV-exposed samples, the data are fit better at shorter times by taking blinking into account, but both recovered the same diffusion times. Blinking was not a factor for the UV-exposed samples, which is expected if particles have aggregated. Diffusion times (τ_{D}) through the confocal volume of 3.09 ± 0.11 ms for the non-UV-exposed QD-DA (i.e., cross-linked by QD-mediated visible-light photocatalysis) and 265 ± 5 ms for the UV-exposed QD-DA were found. These translate into diffusion constants of 20 ± 1 and 0.236 ± 0.004 $\mu m^2/s$, respectively, at the lab temperature of 20 °C. Using the Stokes–Einstein relation in water at 20 °C, these represent hydrodynamic radii of 10 nm for the QD-mediated visible-light cross-linked QD-DA and 900 nm for the UV-exposed QD-DA. On the basis of the sizes of the core–shell QD and the ligand, 10 nm is a reasonable hydrodynamic radius to be expected for single particles, while 900 nm highlights the extensive aggregation of the UV-exposed QD-DA. The lack of aggregation of visible-light cross-linked QD-DA is also evident from the fact that the blinking parameters are needed to fit the data. We also measured the fluorescence lifetime of these samples to determine the extent of fluorescence quenching caused by the aggregation (Supporting Information). The QD-mediated visible-light photocatalysis resulted in cross-linked QDs that show a fluorescence lifetime in water of 9.2 ns, while the UV-exposed QDs show a shorter fluorescence lifetime of 6.9 ns. It is important to reiterate here that no purification step from potential aggregates was performed before taking either of these measurements. The results from this study are schematically depicted in Figure 6, in which using a QD-mediated visible-light cross-linking approach for the ligands was able to both significantly avoid interparticle cross-linking and avoid ligand dissociation that resulted from UV exposure. Ligand dissociation results in QD aggregation over time, while extensive cross-linking of ligands is able to maintain colloidal stability for long periods of time, highlighting the major outcome from this study.

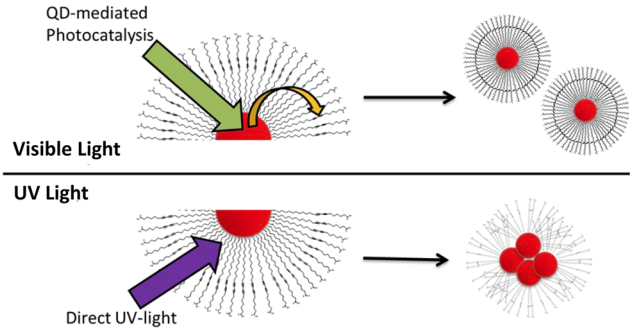

Figure 6. Schematic of the differences observed using our visible-light QD-mediated approach to cross-linking compared to using UV light to directly cross-link the ligands. Under the high energy UV light, ligand dissociation competes with cross-linking that leads to only partial cross-linking of the ligands and eventual aggregation of the QDs.

CONCLUSIONS

We have designed a novel visible-light photo-cross-linking approach to QD long-term stabilization in aqueous solution. This was achieved by synthesizing a photo-cross-linkable diacetylene ligand and using the QD to improve the cross-linking of the ligands on the particle by a visible-light photocatalytic mechanism which, in turn, improved the colloidal properties of the same QD that helped cross-link the ligands. This method combines the advantage of using ligand exchange to render QDs water-soluble with the advantage of controlling cross-linking so that it remains intraparticle rather than interparticle, thus avoiding the formation of aggregates and the need for purification. This new approach has the potential to lead to smaller particle sizes than is possible using amphiphilic polymers by further reducing the size of the bifunctional ligand, although it will be necessary to optimize the correct balance between chain length and SAM packing density to achieve such a goal. Furthermore, other water-soluble bioreactive functionalities can be incorporated, since the cross-linking moiety is completely separated from the bioreactive functional group on the particle, and does not rely on any other reagents added to the solution to achieve the cross-linking.

ASSOCIATED CONTENT

Supporting Information

Synthesis of the diacetylene ligand, PL spectroscopy as a function of UV- and visible-light exposure time, and fluorescence lifetime decay curves for the UV- and visible-light cross-linked DA-QDs. This material is available free of charge via the Internet at http://pubs.acs.org.

AUTHOR INFORMATION

Corresponding Author

*E-mail: cheyes@uark.edu.

Notes

The authors declare no competing financial interest.

ACKNOWLEDGMENTS

C.D.H. would like to thank the NSF (CHE-1255440), NIH (R21 EB009802-01 and COBRE P30 GM103450), and the Arkansas Biosciences Institute for financial support. M.G.G. would like to thank the NSF (CHE-MRI-0922775) for financial support.

REFERENCES

(1) Murray, C. B.; Norris, D. J.; Bawendi, M. G. Synthesis and Characterization of Nearly Monodisperse CdE (E = sulfur, selenium, tellurium) Semiconductor Nanocrystallites. *J. Am. Chem. Soc.* **1993**, *115*, 8706–8715.

(2) Peng, Z. A.; Peng, X. Formation of High-Quality CdTe, CdSe, and CdS Nanocrystals Using CdO as Precursor. *J. Am. Chem. Soc.* **2001**, *123*, 183–184.

(3) Hines, M. A.; Guyot-Sionnest, P. Synthesis and Characterization of Strongly Luminescing ZnS-Capped CdSe Nanocrystals. *J. Phys. Chem.* **1996**, *100*, 468−471.
(4) Woggon, U.; Petri, W.; Dinger, A.; Petillon, S.; Hetterich, M.; Gruen, M.; O'Donnell, K. P.; Kalt, H.; Klingshirn, C. Electronic States And Optical Gain In Strained Cds/Zns Quantum Structures. *Phys. Rev. B: Condens. Matter Mater. Phys.* **1997**, *55*, 1354−1367.
(5) Chan, Y.; Steckel, J. S.; Snee, P. T.; Caruge, J. M.; Hodgkiss, J. M.; Nocera, D. G.; Bawendi, M. G. Blue Semiconductor Nanocrystal Laser. *Appl. Phys. Lett.* **2005**, *86*, 073102/1−073102/3.
(6) Shim, M.; Guyot-Sionnest, P. N-Type Colloidal Semiconductor Nanocrystals. *Nature* **2000**, *407*, 981−3.
(7) Pal, B. N.; Ghosh, Y.; Brovelli, S.; Laocharoensuk, R.; Klimov, V. I.; Hollingsworth, J. A.; Htoon, H. 'Giant' CdSe/CdS Core/Shell Nanocrystal Quantum Dots As Efficient Electroluminescent Materials: Strong Influence of Shell Thickness on Light-Emitting Diode Performance. *Nano Lett.* **2012**, *12*, 331−336.
(8) Kamat, P. V. Quantum Dot Solar Cells. Semiconductor Nanocrystals as Light Harvesters. *J. Phys. Chem. C* **2008**, *112*, 18737−18753.
(9) Bruchez, M.; Moronne, M.; Gin, P.; Weiss, S.; Alivisatos, A. P. Semiconductor Nanocrystals as Fluorescent Biological Labels. *Science* **1998**, *281*, 2013−2016.
(10) Chan, W. C.; Nie, S. Quantum Dot Bioconjugates for Ultrasensitive Nonisotopic Detection. *Science* **1998**, *281*, 2016−2018.
(11) Petryayeva, E.; Algar, W. R.; Medintz, I. L. Quantum Dots in Bioanalysis: A Review of Applications Across Various Platforms for Fluorescence Spectroscopy and Imaging. *Appl. Spectrosc.* **2013**, *67*, 215−252.
(12) Campos, B. B.; Algarra, M.; Alonso, B.; Casado, C. M.; Esteves, d. S. J. C. G. Mercury(II) Sensing Based On The Quenching Of Fluorescence Of Cds-Dendrimer Nanocomposites. *Analyst* **2009**, *134*, 2447−2452.
(13) Liu, Y.; Brandon, R.; Cate, M.; Peng, X.; Stony, R.; Johnson, M. Detection of Pathogens Using Luminescent CdSe/ZnS Dendron Nanocrystals And A Porous Membrane Immunofilter. *Anal. Chem.* **2010**, *79*, 8796−802.
(14) Omogo, B.; Aldana, J.; Heyes, C. D. Radiative and Nonradiative Lifetime Engineering of Quantum Dots in Multiple Solvents by Surface Atom Stoichiometry and Ligands. *J. Phys. Chem. C* **2013**, *117*, 2317−2327.
(15) Nida, D. L.; Nitin, N.; Yu, W. W.; Colvin, V. L.; Richards-Kortum, R. Photostability of Quantum Dots With Amphiphilic Polymer-Based Passivation Strategies. *Nanotechnology* **2008**, *19*, 035701.
(16) Anderson, R. E.; Chan, W. C. W. Systematic Investigation of Preparing Biocompatible, Single, and Small ZnS-Capped CdSe Quantum Dots with Amphiphilic Polymers. *ACS Nano* **2008**, *2*, 1341−1352.
(17) Michalet, X.; Pinaud, F. F.; Bentolila, L. A.; Tsay, J. M.; Doose, S.; Li, J. J.; Sundaresan, G.; Wu, A. M.; Gambhir, S. S.; Weiss, S. Quantum Dots for Live Cells, in Vivo Imaging, and Diagnostics. *Science* **2005**, *307*, 538−544.
(18) Yu, W. W.; Chang, E.; Drezek, R.; Colvin, V. L. Water-soluble Quantum Dots For Biomedical Applications. *Biochem. Biophys. Res. Commun.* **2006**, *348*, 781−786.
(19) Zhang, Y.; Clapp, A. Overview of Stabilizing Ligands for Biocompatible Quantum Dot Nanocrystals. *Sensors* **2011**, *11*, 11036−11055.
(20) Breus, V. V.; Heyes, C. D.; Nienhaus, G. U. Quenching of CdSe-ZnS Core-Shell Quantum Dot Luminescence by Water-Soluble Thiolated Ligands. *J. Phys. Chem. C* **2007**, *111*, 18589−18594.
(21) Clapp, A. R.; Goldman, E. R.; Mattoussi, H. Capping of CdSe-ZnS Quantum Dots With DHLA And Subsequent Conjugation With Proteins. *Nat. Protoc.* **2006**, *1*, 1258−66.
(22) Takeuchi, H.; Omogo, B.; Heyes, C. D. Are Bidentate Ligands Really Better than Monodentate Ligands For Nanoparticles? *Nano Lett.* **2013**, *13*, 4746−4752.
(23) Aldana, J.; Lavelle, N.; Wang, Y.; Peng, X. Size-Dependent Dissociation pH of Thiolate Ligands from Cadmium Chalcogenide Nanocrystals. *J. Am. Chem. Soc.* **2005**, *127*, 2496−2504.
(24) Jeong, S.; Achermann, M.; Nanda, J.; Ivanov, S.; Klimov, V. I.; Hollingsworth, J. A. Effect of the Thiol-Thiolate Equilibrium on the Photophysical Properties of Aqueous CdSe/ZnS Nanocrystal Quantum Dots. *J. Am. Chem. Soc.* **2005**, *127*, 10126−10127.
(25) Kim, S.-W.; Kim, S.; Tracy, J. B.; Jasanoff, A.; Bawendi, M. G. Phosphine Oxide Polymer for Water-Soluble Nanoparticles. *J. Am. Chem. Soc.* **2005**, *127*, 4556−4557.
(26) Jiang, W.; Mardyani, S.; Fischer, H.; Chan, W. Design and Characterization Of Lysine Cross-Linked Mercapto-Acid Biocompatible Quantum Dots. *Chem. Mater.* **2006**, *18*, 872−878.
(27) Kim, T.; Ye, Q.; Sun, L.; Chan, K. C.; Crooks, R. M. Polymeric Self-Assembled Monolayers. 5. Synthesis and Characterization of ω-Functionalized, Self-Assembled Diacetylenic and Polydiacetylenic Monolayers. *Langmuir* **1996**, *12*, 6065−6073.
(28) Alloisio, M.; Demartini, A.; Cuniberti, C.; Muniz-Miranda, M.; Giorgetti, E.; Giusti, A.; Dellepiane, G. Photopolymerization of Diacetylene-Capped Gold Nanoparticles. *Phys. Chem. Chem. Phys.* **2008**, *10*, 2214−2220.
(29) Harris, C.; Kamat, P. Photocatalysis with CdSe Nanoparticles in Confined Media: Mapping Charge Transfer Events in the Subpicosecond to Second Timescales. *ACS Nano* **2009**, *3*, 682−690.
(30) Sill, K.; Emrick, T. Nitroxide-mediated Radical Polymerization From CdSe Nanoparticles. *Chem. Mater.* **2004**, *16*, 1240−1243.
(31) Barichard, A.; Galstian, T.; Israeli, Y. Physico-chemical Role of CdSe/ZnS Quantum Dots In The Photo-Polymerization Process Of Acrylate Composite Materials. *Phys. Chem. Chem. Phys.* **2012**, *14*, 8208−8216.
(32) Xu, Z. C.; Byun, H. S.; Bittman, R. Synthesis of Photopolymerizable Long-Chain Conjugated Diacetylenic Acids and Alcohols from Butadiyne Synthons. *J. Org. Chem.* **1991**, *56*, 7183−7186.
(33) Kim, T.; Crooks, R. M. Polymeric Self-Assembling Monolayers 0.1. Synthesis and Characterization of Omega-Functionalized N-Alkanethiols Containing a Conjugated Diacetylene Group. *Tetrahedron Lett.* **1994**, *35*, 9501−9504.
(34) Omogo, B.; Aldana, J. F.; Heyes, C. D. Radiative and Nonradiative Lifetime Engineering of Quantum Dots in Multiple Solvents by Surface Atom Stoichiometry and Ligands. *J. Phys. Chem. C* **2013**, *117*, 2317−2327.
(35) Durisic, N.; Godin, A. G.; Grutter, P.; Wiseman, P. W.; Heyes, C. D. Probing the "Dark" Fraction of Core−Shell Quantum Dots by Ensemble and Single Particle pH-Dependent Spectroscopy. *ACS Nano* **2011**, *5*, 9062−9073.
(36) Aldana, J.; Wang, Y. A.; Peng, X. Photochemical Instability of CdSe Nanocrystals Coated By Hydrophilic Thiols. *J. Am. Chem. Soc.* **2001**, *123*, 8844−50.
(37) http://webbook.nist.gov/cgi/cbook.cgi?ID=C2809690&Units=SI&Mask=80#Refs.
(38) Schmidtke, C.; Lange, H.; Tran, H.; Ostermann, J.; Kloust, H.; Bastus, N.; Merkl, J.; Thomsen, C.; Weller, H. Radical Initiated Reactions on Biocompatible CdSe-Based Quantum Dots: Ligand Cross-Linking, Crystal Annealing, and Fluorescence Enhancement. *J. Phys. Chem. C* **2013**, *117*, 8570−8578.
(39) Heuff, R. F.; Swift, J. L.; Cramb, D. T. Fluorescence correlation Spectroscopy Using Quantum Dots: Advances, Challenges And Opportunities. *Phys. Chem. Chem. Phys.* **2007**, *9*, 1870−1880.
(40) Heyes, C. D.; Kobitski, A. Y.; Breus, V. V.; Nienhaus, G. U. Effect of the Shell on Blinking Statistics in Single Core-Shell Quantum Dots - A Single Particle Fluorescence Study. *Phys. Rev. B* **2007**, *75*, 125431.

NOTE ADDED AFTER ASAP PUBLICATION

This paper published ASAP on July 28, 2014. A change was made to Figure 5 caption and the revised version was reposted on July 29, 2014.